Chalcogenide Letters Vol. 20, No. 9, September 2023, p. 629 - 637

The effects of thickness and doping concentration on the solar efficiency of GaN/p-Si based solar cells

N. S. Khairuddin[a], M. Z. Mohd Yusoff[a,*], H. Hussin[b]
[a]*School of Physics and Material Studies, Faculty of Applied Sciences, Universiti Teknologi MARA, 40450 Shah Alam, Selangor, Malaysia*
[b]*School of Electrical Engineering, College of Engineering, Universiti Teknologi MARA, 40450 Shah Alam, Selangor, Malaysia*

In this study, we used the PC1D simulator to demonstrate the performance analysis of a solar cell model based on gallium nitride (GaN). It has been discovered that when the layer thickness of the GaN substrate grows, the efficiency of solar cells decreases. This was found by comparing the doping concentration and layer thickness on the GaN and silicon substrates. As the thickness of the p-doping Si layer rises, cell efficiency increases just modestly. The optimal doping concentrations for GaN and p-silicon are $1x10^{18}$ cm^{-3} and $1x10^{17}$ cm^{-3}, respectively. In compared to other designs, GaN/p-silicon solar cells have the highest efficiency of 25.26%.

(Received June 21, 2023; Accepted September 1, 2023)

Keywords: Solar cell, GaN, Gallium Nitride, Silicon, PC1D

1. Introduction

Gallium Nitride (GaN) devices are naturally gaining market share. GaN revenues will expand with a cumulative annual growth rate of 75% over the following five years, according to market forecast [1]. Power electronics experts are currently confronted with issues relating to the circuit design technique, passive component selection, thermal management, and experimental testing due to its high switching speed and operational switching frequency [2]. For applications in optoelectronics and microelectronics, III-V nitrides like gallium nitride (GaN), aluminium nitride (AlN), and indium nitride (InN), as well as their alloys, are particularly appealing. GaN alloys have an adjustable direct gap, which is why photovoltaics use them. Their bandgap is one of the most alluring places at first [3]. Si was also intended to incorporate as an n-type dopant in the low-temperature plasma-enhanced chemical vapor deposition (PECVD) method since it is a well-known donor dopant in high-temperature GaN [4]. Due to its direct bandgap (Eg~ 3.4 eV), transmittance exceeding 82% across the entire visible spectrum, high electron mobility (~1,000 cm2/Vs) [5], high thermal conductivity, and excellent chemical stability [6], gallium nitride (GaN) has excellent optical and electrical properties. The InGaN material system's band gap now spans the infrared to ultraviolet spectrum. The InGaN material system is advantageous for photovoltaic applications because it can be used to fabricate third-generation devices like intermediate-band solar cells, in addition to high-efficiency multijunction solar cells, due to its direct and wide band gap ranges [7]. The nitrides exhibit advantageous photovoltaic properties like low effective mass of carriers, high mobilities, high peak and saturation velocities, high absorption coefficients, and radiation tolerance in addition to the wide band gap range [8]. Its potential for high-efficiency photovoltaics is confirmed by the III-V nitrides technology's ability to grow high-quality crystalline structures and create optoelectronic devices [9]. Fermi level moves upward obviously as GaN thickness rises, along with a decrease in the conduction band minimum (CBM) value and an increase in the valance band maximum (VBM) value [10]. The relaxation of compressive stress and increase in carrier concentration for a thicker GaN layer is a preliminary explanation for the thickness-dependent band structure [11]. The aforementioned circumstance enables us to control

* Corresponding author: zaki7231@uitm.edu.my
https://doi.org/10.15251/CL.2023.209.629

the GaN layer's energy level through thickness control, accelerating its use in next-generation solar cells [12].

Typically, foreign substrates like SiC, Al_2O_3, and Si are used to grow GaN-based devices. Although the growth onto these substrates is accompanied by a number of deep-level defects, such as dislocations brought on by thermal, lattice, and strain (tensile or compressive) differences, these defects may limit the consistency and applicability of GaN-based devices [13]. The performance of the device is negatively impacted by leakage current in the space charge region, which is caused by these defects, which also result in trap energy levels (recombination centers) for both electron and hole charge carriers [14]. A buffer layer between the Si and the active layer has been used by many researchers to grow GaN-based devices on Si in order to minimise GaN layer flaws. However, the use of buffer layers results in heterojunction failure and moderated vertical conductions. Additionally, it has been found that manufacturing firms are more profitable when Si electronics are combined with GaN-based photonic devices. Reducing device costs and simultaneously integrating GaN-based devices with Si electronics on the same chip is critical for the success of the GaN-based optoelectronics industry. Studies have shown that there is a significant effort being made to use a variety of growth techniques to grow GaN materials on Si chips for integrated devices. The development of single GaN-based heterojunctions for solar cell applications has drawn more attention due to their potential for higher conversion efficiency and lower production costs in the context of solar cell applications. To improve the performance of GaN/Si heterojunction solar cells, it is therefore necessary to tune the growth conditions, such as pressure, deposition rate, and growth temperature [15]. The IV curves of the solar cells that were simulated in the PC1D program resembled those that were discovered through experimentation, although certain differences were apparent, revealing a clear discrepancy between the parameters discovered experimentally and those discovered virtually [16].

A numerical simulation tool, like the PC1D simulation tool, is used to simulate photovoltaic solar cells and complement experimental data. A number of numerical simulations of crystalline solar cells conducted by the photovoltaic (PV) community showed PC1D the positive effects of PV technology. A number of PCID simulations were performed on various solar cell structures, including bifacial solar cells and silicon-based monocrystalline solar cells, and their effects on key parameters, including the amount of emitter doping, wafer thickness, front and rear recombination, and bulk doping, were discovered to be important [17]. A lot of libraries files for the bandgap, refractive index, dielectric constant, electron affinity, electron-hole mobilities, doping concentration, carrier lifetimes, etc. for GaAs, Ge, GIN, InP, c-Si, a-Si, and AlGaAs based devices are available in PC1D, which enables simulation of various semiconductor device properties [18]. In order to minimise costs while maximising device efficiency, careful selection of materials with the ideal thickness and doping levels is crucial [19]. The advantages of reduced parasitic absorption from the wide gap between the GaN layers must be fully realized in order to develop effective doping techniques [20]. The benefit of using numerical modeling tools, like PC1D, to optimise the emitter designs is that doing so requires less money, time, and effort than analysing the effects of changing the configuration of the solar cells [21].

2. Experimental work

The simulated hetero structure consists of GaN and Si which have a band gap of 3.42 eV and 1.124 eV, respectively. The active area of GaN/p-Si based solar cell is set to 100 cm^2 as shown in Figure 1. The numerical simulation Personal Computer One Dimensional (PC1D) is used to study electrical and optical properties of GaN/p-Si solar cells.

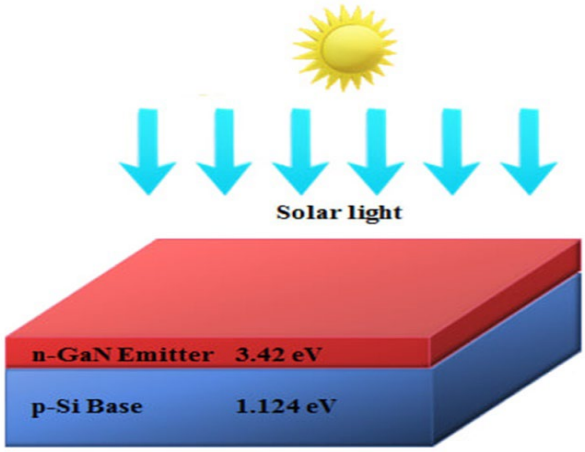

Fig. 1. Simulation structure of GaN/p-Si based solar cell.

In PC1D simulation software, gallium nitride and silicon are assigned as the n-region layer and p-region layer, respectively. The effect of various n and p regions thicknesses and doping concentrations on the GaN/p-Si based solar cell performance are investigated in this work. Table 1 provides a description of the model parameters used in this work. Figure 2 indicates the values filled in for the fundamental variables used to simulate a GaN/p-Si based solar cell. The PC1D simulation is conducted to determine the short circuit current (I_{sc}), open circuit voltage (V_{oc}), and maximum output power (P_{max}). Fill factor (FF) and efficiency (η) will be determined based on the outcome.

Table 1. Basic parameters used in the simulation of GaN/p-Si based solar cells

Parameter	**Value**	
Device area	$100cm^2$	
Region	n-GaN layer	p-Si layer
Thickness	0.1 µm	160 µm
Band gap	3.42 eV	1.124 eV
Intrinsic conc. (300K)	$2.35\times10^{-15}cm^{-3}$	$1\times10^{10}cm^{-3}$
Background doping	$1\times10^{16}cm^{-3}$	$1\times10^{16}cm^{-3}$
Bulk recombination lifetime	2×10^{-3} µs	1000 µs
Excitation mode	One-sun (transient; 16 timesteps)	
Spectrum	AM1.5G	
Intensity	$0.1W/cm^2$	
Temperature	25°C	

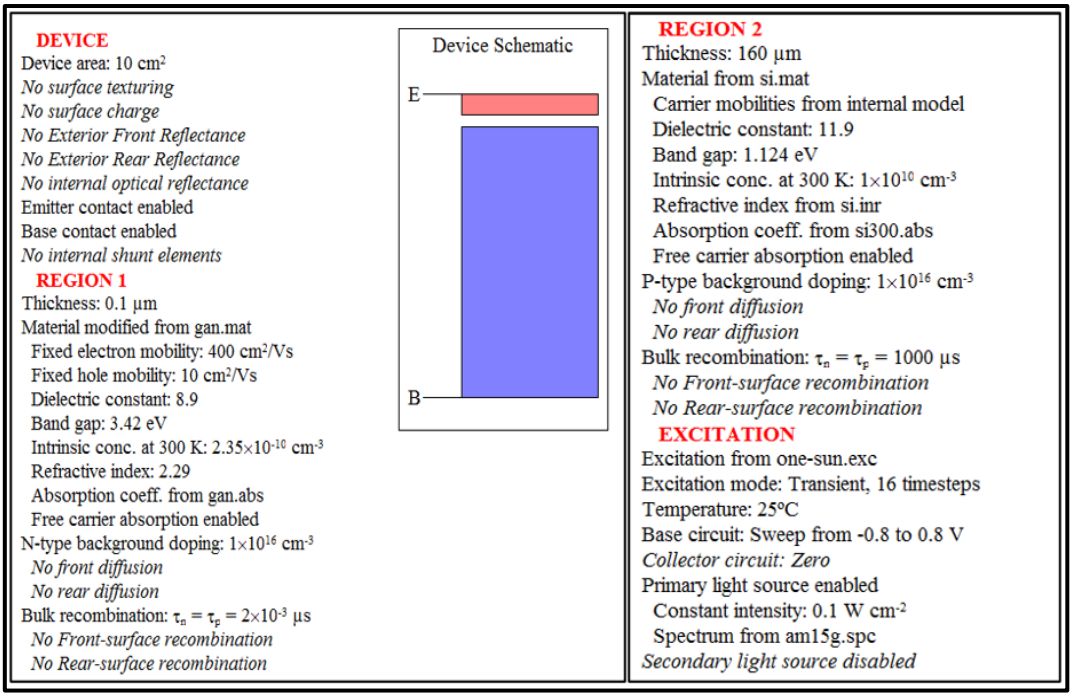

Fig. 2. Basic parameters used in PC1D simulation of GaN/p-Si based solar cell.

3. Result and discussion

The simulation findings for gallium nitride with silicon (GaN/p-Si) solar cells using the PC1D program are discussed in this section. The performance of GaN/p-Si solar cell was investigated by changing the thickness of the n- and p-regions, as well as doping concentration for both layers. The device performance of all parameters can be viewed in terms of I_{sc}, V_{oc}, P_{max}, fill factor (FF), IV characteristic and efficiency (η). Figure 3 shows the effect of various thickness of GaN layer in GaN/p-Si solar cells. The thickness of GaN layer was changed from 0.1 to 0.5 µm. Figure 3 illustrates that changing the thickness of an n-region GaN/p-Si solar cell can affect its efficiency. The Figure 3 (inset) shows that the highest curve corresponds to the thinnest layer of GaN (0.1 nm).

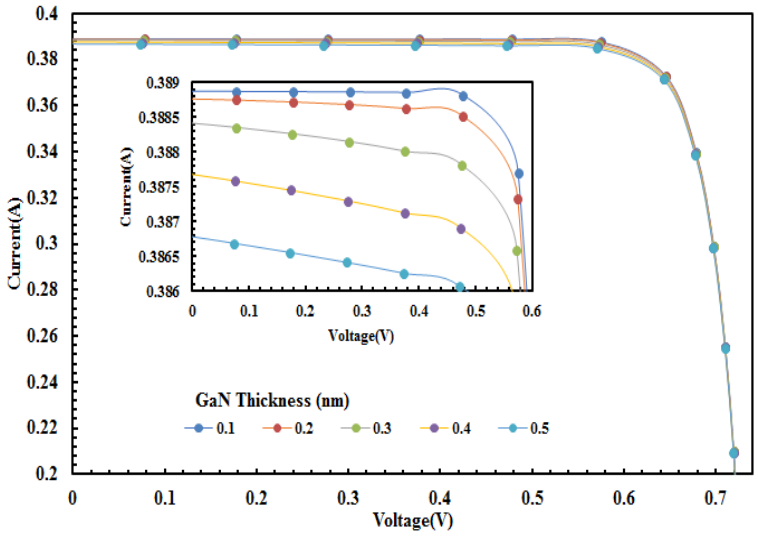

Fig. 3. The effect of various thicknesses of n-region at GaN/p-Si solar cell.

Table 2 demonstrates that the reduced efficiency with the increasing of GaN thickness from 24.11% η at 0.1µm to 23.93% η at 0.5µm. This demonstrates that the changes of GaN thickness influenced all the cell parameters, as the value obtained fixed at the short circuit (I_{sc}) was followed by an increase in the value of the open circuit voltage (V_{oc}) and fill factor (FF), and thus an increase in the value of the conversion efficiency (%), as they are directly proportional, to accelerate the rate of energy absorption.

Table 2. Output parameters on different thickness at n-region GaN/P-Si solar cell.

N-region Thickness, (µm)	I_{sc} (A)	V_{oc} (V)	P_{max} (W)	Fill Factor (FF)	Efficiency, η (%)
0.1	0.3889	0.7417	0.2411	0.8358	24.11
0.2	0.3888	0.7417	0.2408	0.8350	24.08
0.3	0.3884	0.7416	0.2402	0.8339	24.02
0.4	0.3877	0.7416	0.2397	0.8336	23.97
0.5	0.3868	0.7415	0.2393	0.8343	23.93

The optimal efficiency of the GaN/p-Si solar cell was attained at the thinnest possible layer in the n-region, which is 0.1µm at 24.11% efficiency with V_{oc} = 0.7417V, I_{sc} =0.3889A, P_{max} = 0.2411W and FF = 0.8359. The effects of increasing layer thickness led the outcomes to inversely decrease and efficiency to gradually decrease [22]. The impact of silicon thickness on the GaN/p-Si Solar Cell was presented in this work. The influence of thicknesses at the silicon substrate on the performance of the GaN/p-Si solar cell is depicted in Figure 4. The result shows that the varied thickness of silicon substrate in GaN/p-Si based solar cells can affect their efficiency. The highest current value is obtained when the thickness of the GaN substrate is 0.1m and the lowest value is obtained when the thickness is 0.5m, as shown in Figure 4 (inset). The effects of increase of layer thickness at p-region were gradual increase the efficiency [23]. In reference to the curves of p-region of GaN/p-Si solar cell, the efficiency shows a decline in efficiency as the thickness increases from 30µm to 150µm. The lower value of current occurs to the thickness of 30µm, and the highest value of current occurs to the thickness of 150µm. The limitation in this parameter was uncovered using PC1D. When the p-region thickness exceeded 300µm, the power diminished.

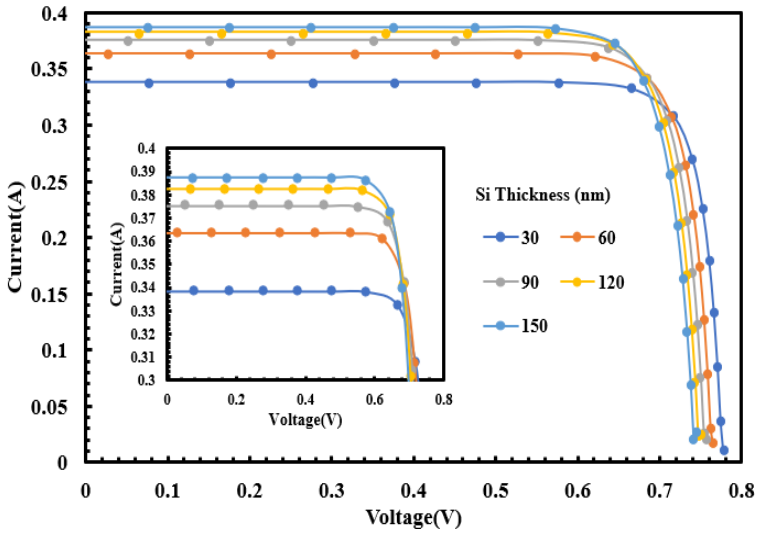

Fig. 4. The influence of thickness at p-region GaN/P-Si solar cell.

The optimal efficiency of the GaN/p-Si solar cell was attained at the thickest layer in the silicon substrate, which is 150µm at 24.10% efficiency with V_{oc} = 0.7433V, I_{sc} =0.3875A, P_{max} = 0.241W and FF = 0.8367, as shown in Table 3.

Table 3. Output parameters on different thickness at P-region GaN/p-Si solar cell.

P-region Thickness, (µm)	I_{sc} (A)	V_{oc} (V)	P_{max} (W)	Fill Factor (FF)	Efficiency, η (%)
30	0.3384	0.7768	0.2243	0.853276338	22.43
60	0.3638	0.7636	0.2341	0.842699622	23.41
90	0.3754	0.7551	0.2384	0.841022302	23.84
120	0.3826	0.7486	0.2403	0.838994246	24.03
150	0.3875	0.7433	0.241	0.836722029	24.1

This study additionally looks at the effect of different doping concentrations on GaN/p-Si-based solar cells. The concentration of the substrate also plays an essential role in efficiency estimates. Figure 5 shows the result for the influence of doping concentration at GaN substrate. The n-region doping concentration was observed over five orders of magnitude from $1x10^{15}$ cm^{-3} to $1x10^{19}$ cm^{-3} respectively.

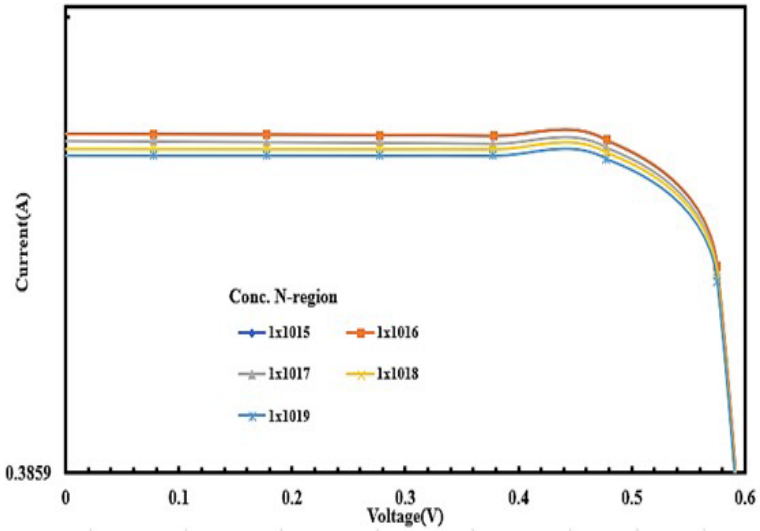

Fig. 5. IV characteristic for the influence of doping concentration at GaN substrate.

Results from various doping concentration (from $1x10^{15}$ to $1x10^{18}$ cm^{-3}) at GaN substrate show the same efficiency value. Besides, the solar efficiency starts to diminish owing to recombination in the severely doped emitter layer at doping level of $1\times10^{19}cm^{-3}$. Therefore, the doping concentration of the n-region GaN/p-Si solar cell optimized as $1x10^{18}$ cm^{-3}.

Table 4. Output parameters on different doping concentration at n-region GaN/p-Si solar cell.

N-region doping concentration, (cm^{-3})	I_{sc} (A)	V_{oc} (V)	P_{max} (W)	Fill Factor (FF)	Efficiency, η (%)
$1x10^{15}$	0.3889	0.7417	0.2411	0.8358551	24.11
$1x10^{16}$	0.3889	0.7417	0.2411	0.8358551	24.11
$1x10^{17}$	0.3888	0.7417	0.2411	0.8360701	24.11
$1x10^{18}$	0.3887	0.7417	0.2411	0.8362852	24.11
$1x10^{19}$	0.3887	0.7417	0.241	0.8359383	24.10

As shown in Table 4, a similar efficiency (24.11%) of GaN/p-Si solar cell was achieved when n type doping concentration were set at 1×10^{15} cm^{-3}, 1×10^{16} cm^{-3}, 1×10^{17} cm^{-3}, and 1×10^{18} cm^{-3}. Figure 6 shows the electrical properties for various doping concentration at p-type silicon substrate. The p-region doping concentration of silicon substrates were changed over five orders of magnitude from 1×10^{14} to 1×10^{18} cm^{-3}. The highest efficiency of GaN/p-silicon solar cells is recorded as 25.26% when $1\times10^{17}cm^{-3}$ is used (refer to Figure 6 (inset)). The short circuit current drop with a rise in acceptor density, the saturation current of the device increases with acceptor concentration, which elevates the V_{oc}. However, the short circuit current drop at the concentration of $1\times10^{17}cm^{-3}$.

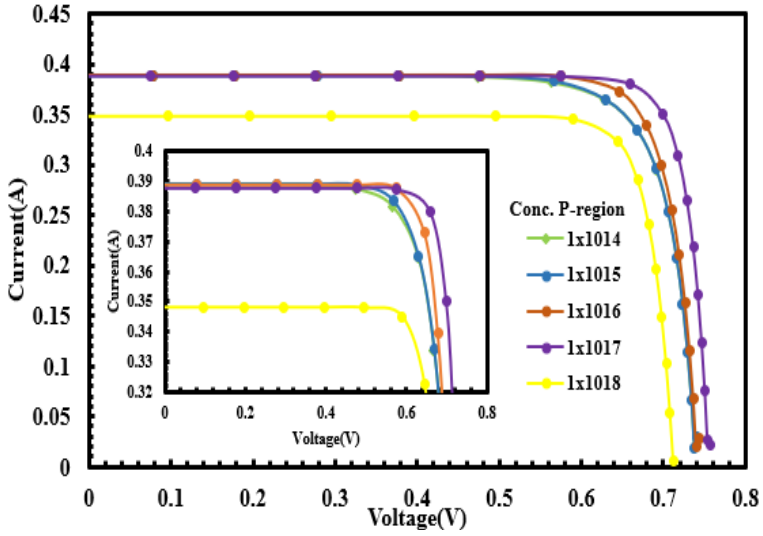

Fig. 6. The influence of doping concentration at p-region GaN solar cell.

Table 5. Output parameters on different doping concentration at p-region GaN/p-Si solar cell.

P-region doping concentration, (cm^{-3})	I_{sc} (A)	V_{oc} (V)	P_{max} (W)	Fill Factor (FF)	Efficiency, η (%)
$1x10^{14}$	0.3890	0.7385	0.2295	0.7988	22.95
$1x10^{15}$	0.3889	0.7388	0.23	0.8005	23
$1x10^{16}$	0.3889	0.7417	0.2411	0.8358	24.11
$1x10^{17}$	0.3879	0.7555	0.2526	0.8619	25.26
$1x10^{18}$	0.3479	0.7125	0.2091	0.8435	20.91

The optimal efficiency of the p-region doping concentration of GaN/p-Si solar cell was attained at $1x10^{17}cm^{-3}$ with 25.26% efficiency with V_{oc} = 0.7555V, I_{sc} = 0.3879A, P_{max} = 0.2526W and FF = 0.8619. Figure 7 depicts the PV and IV characteristics. GaN/p-Si solar cells are capable to reach a higher efficiency of 25.26% when these optimal circumstances are applied.

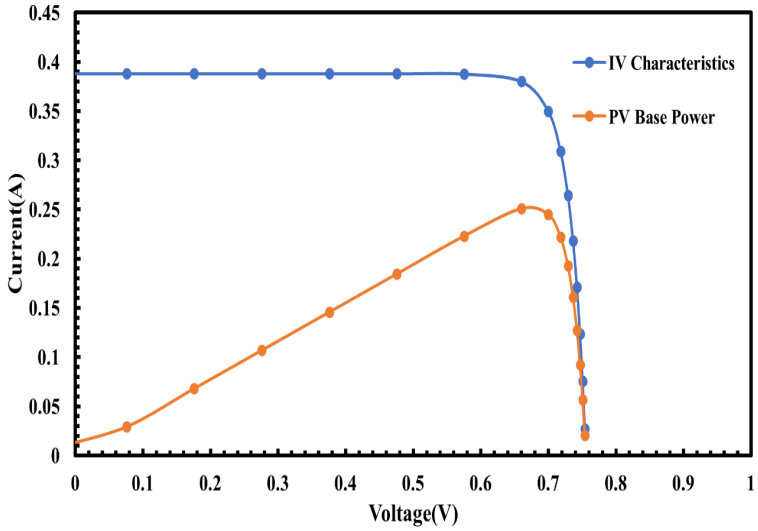

Fig. 7. Graph of IV and PV curves.

4. Conclusion

In summary, we successfully simulated a greater efficiency of GaN/p-silicon substrate using numerical simulation PC1D software. We discovered that the efficiency reduces dramatically as the layer thickness of the GaN substrate increases. Furthermore, as silicon thickness increases, it also improves the efficiency of solar cells. When the concentration of n-type doping in solar cells is altered, the efficiency remains constant. However, the efficiency changes slightly when p-type doping in the silicon layer increases. The ideal doping concentrations for GaN and p-silicon are $1x10^{18}$ cm^{-3} and $1x10^{17}$ cm^{-3}, respectively. In comparison to other designs, GaN/p-silicon solar cells have the greatest efficiency of 25.26%.

Acknowledgments

The financial support from Universiti Teknologi MARA is gratefully acknowledged.

References

[1] Iannaccone, G., Sbrana, C., Morelli, I., & Strangio, S. IEEE Access, 9, 139446-139456 (2021); https://doi.org/10.1109/ACCESS.2021.3118897

[2] Dalla Vecchia, M., Ravyts, S., Van den Broeck, G., & Driesen, J. Energies, 12(14), 2663 (2019); https://doi.org/10.3390/en12142663

[3] Mazari, H., Ameur, K., Boumesjed, A., Benseddik, N., Benamara, Z., & Benyahya, N. Nanotechnology, 257-264 (2021).

[4] Fioretti, A. N., Chien, T. C. C., Xiao, Y., Ballif, C., & Boccard, M. (pp. 2608-2612). IEEE (2019).

[5] Lee, K. J., Min, J. W., Turedi, B., Alsalloum, A. Y., Min, J. H., Kim, Y. J., ... & Bakr, O. M.

ACS Energy Letters, 5(10), 3295-3303 (2020); https://doi.org/10.1021/acsenergylett.0c01621

[6] Qiu, P., Wei, H., An, Y., Wu, Q., Du, W., Jiang, Z., Zheng, X. Ceramics International, 46(5), 5765-5772 (2020); https://doi.org/10.1016/j.ceramint.2019.11.026

[7] García de Arquer, F. P., Talapin, D. V., Klimov, V. I., Arakawa, Y., Bayer, M., & Sargent, E. H. Science, 373(6555), eaaz8541 (2021); https://doi.org/10.1126/science.aaz8541

[8] Chen, J., Ouyang, W., Yang, W., He, J. H., & Fang, X. Advanced Functional Materials, 30(16), 1909909 (2020); https://doi.org/10.1002/adfm.201909909

[9] Jani, O., Ferguson, I., Honsberg, C., & Kurtz, S. Applied Physics Letters, 91(13), 132117 (2007); https://doi.org/10.1063/1.2793180

[10] Lev, L. L., Maiboroda, I. O., Grichuk, E. S., Chumakov, N. K., Schröter, N. B. M., Husanu, M. A., & Strocov, V. N. Physical Review Research, 4(1), 013183 (2022); https://doi.org/10.1103/PhysRevResearch.4.013183

[11] Wang, J., Shu, H., Liang, P., Zhou, X., Cao, D., & Chen, X. Computational Materials Science, 172, 109337 (2020); https://doi.org/10.1016/j.commatsci.2019.109337

[12] Deshmukh, M. A., Park, S. J., Hedau, B. S., & Ha, T. J. Solar Energy, 220, 953-990 (2021); https://doi.org/10.1016/j.solener.2021.04.001

[13] Wu, N., Xing, Z., Li, S., Luo, L., Zeng, F., & Li, G. Semiconductor Science and Technology, 38(6), 063002 (2023); https://doi.org/10.1088/1361-6641/acca9d

[14] Qi, F., Deng, X., Wu, X., Huo, L., Xiao, Y., Lu, X., & Jen, A. K. Y. Advanced Energy Materials, 9(42), 1902600 (2019); https://doi.org/10.1002/aenm.201902600

[15] Saron, K. M. A., Ibrahim, M., Hashim, M. R., Taha, T. A., Elfadill, N. G., Mkawi, E. M., & Allam, N. K. Applied Physics Letters, 118(2), 023902 (2021); https://doi.org/10.1063/5.0037866

[16] Rodríguez-Castro, S., Álvarez-Macías, C., Santana-Rodríguez, G., Dutt, A., Hernández-Jacobo, C., & Loera-Palomo, R. In 2020 47th IEEE Photovoltaic Specialists Conference (PVSC) (pp. 0540-0543). IEEE (2020).

[17] Kumar, S. G., Shetty, A. P., & Prashanth, C. R. 2nd International Conference for Emerging Technology (INCET) (pp. 1-6). IEEE (2021).

[18] Shah, D. K., Devendra, K. C., Kim, T. G., Akhtar, M. S., Kim, C. Y., & Yang, O. B. Optical Materials, 121, 111500 (2021); https://doi.org/10.1016/j.optmat.2021.111500

[19] Bouadi, A., Naim, H., Djelloul, A., Benkrima, Y., & Fares, R. Chalcogenide Letters, 19(9), 611-619 (2022); https://doi.org/10.15251/CL.2022.199.611

[20] Amano, H., Collazo, R., De Santi, C., Einfeldt, S., Funato, M., Glaab, J., & Zhang, Y. Journal of Physics D: Applied Physics, 53(50), 503001 (2020); https://doi.org/10.1088/1361-6463/aba64c

[21] Clugston, D. A., & Basore, P. A. PC1D version 5: 32-bit solar cell modeling on personal computers. In Conference Record of the Twenty Sixth IEEE Photovoltaic Specialists Conference-1997 (pp. 207-210). IEEE (1997).

[22] Mohamed, E. T., Maka, A. O., Mehmood, M., Direedar, A. M., & Amin, N. Sustainable Energy Technologies and Assessments, 44, 101067 (2021); https://doi.org/10.1016/j.seta.2021.101067

[23] Wang, W. J., Liao, M. L., Yuan, J., Luo, S. Y., & Huang, F. Chinese Physics B, 31(7), 074206 (2022); https://doi.org/10.1088/1674-1056/ac597c